Bulletin of Engineering Geology and the Environment (2021) 80:5675–5692
https://doi.org/10.1007/s10064-021-02254-x

ORIGINAL PAPER

Back analysis of surrounding rock parameters of tunnel considering displacement loss and space effect

Yong Zhao[1] · Shi-Jin Feng[1]

Received: 6 October 2020 / Accepted: 19 April 2021 / Published online: 29 April 2021

Abstract

Displacement back analysis is often performed to estimate rock parameters in tunnel construction. However, most researchers use the final values of monitoring displacement without considering the loss involved and the space effect, causing substantial errors. In this study, a displacement-based back analysis method is developed for estimating rock parameters, and both the displacement loss and space effect are considered when selecting and processing the output data of the algorithm. The method involves the following steps: First, reasonable training samples are set through numerical simulation, sensitivity analysis, and orthogonal design. Next, an extreme learning machine (ELM) optimized using particle swarm optimization (PSO) is trained to replace the time-consuming numerical analysis. Finally, the PSO algorithm is again utilized to determine the optimal parameters, and the displacement loss is calculated. The results of a simulation case indicate that the proposed method is highly precise and can be generalized adequately. The prediction accuracy can be improved by selecting rock parameters with high sensitivities and the typical monitoring data. An engineering application in the Jigongshan Tunnel in Shenzhen, China, demonstrates that this method can offer a reliable reference in terms of rock parameters to fulfill practical engineering demands, and provide an alternative approach for ground stress estimation during tunneling.

Keywords Displacement back analysis · Displacement loss · Space effect · Extreme learning machine · Particle swarm optimization

Introduction

During tunnel design and construction, it is crucial to determine the initial state of stress and underground material properties, for both understanding the structural behavior and modeling the construction area numerically (Sakurai and Takeuchi 1983). However, owing to the nonhomogeneous characteristics of the ground and uncertainties in exploration, these rock or soil parameters can only be identified within limited scope, and the values obtained from field or laboratory tests cannot be used directly for further analysis. Accidents have occurred occasionally because of the use of inappropriate parameters in tunnel design (Hoek and Diederichs 2006; Cai 2011; Zhang et al. 2020b).

The reliability of tunnel design parameters can be verified through field monitoring (Liu and Liu 2019). Further, the displacement, as the most common monitoring index in tunnel construction, can be a good base for the back analysis of rock or soil parameters. Ever since the first paper on displacement-based back analysis was published (Kavanagh and Clough 1971), this method has been used to estimate the following:

- Basic mechanical rock or soil parameters (Feng et al. 2000; Fakhimi et al. 2004; Yazdani et al. 2012; Shreedharan and Kulatilake 2015; Kang et al. 2017)

Highlights
- A displacement-based back analysis method that considers the displacement loss and space effect is proposed to predict rock parameters in tunnel construction.
- The extreme learning machine (ELM) and particle swarm optimization (PSO) are combined to replace numerical analysis and search for the optimal solution.
- Measures are provided to improve the quality of training samples and the precision of the algorithm.
- The advantages, limitations, and prospects of the proposed method are discussed.

✉ Shi-Jin Feng
fsjgly@tongji.edu.cn

Yong Zhao
1810023@tongji.edu.cn

[1] Key Laboratory of Geotechnical and Underground Engineering of the Ministry of Education, Department of Geotechnical Engineering, Tongji University, Shanghai 200092, China

- Rheological parameters (Sharifzadeh et al. 2013; Qi and Fourie 2018; Zhang et al. 2020b)
- Seepage parameters (Wu et al. 2019)
- Parameters of rock or soil constitutive model (Rechea et al. 2008; Gao et al. 2020)
- In situ stress (Kaiser et al. 1990; Gao and Ge 2016; Bertuzzi 2017; Xu and Ni 2019)

Generally, back analysis techniques based on displacement can be classified into three categories (Qi and Fourie 2018): (1) analytical or semi-analytical methods (Bertuzzi 2017; Zhang et al. 2017); (2) numerical modeling (Zhang et al. 2006; Hisatake and Hieda 2008; Luo et al. 2018), and (3) statistical learning (Huang et al. 2011; Song et al. 2015; Gao and Ge 2016; Liu and Liu 2019; Zhang et al. 2020b). In analytical or semi-analytical methods, assumptions and simplifications are often made to obtain feasible solutions, resulting in the restricted applicability of such methods in practical engineering cases. Numerical methods are widely utilized to calculate the displacement, and the input parameters for numerical models can be estimated through trial-and-error or other optimization algorithms (Hisatake and Hieda 2008; Manzanal et al. 2016). However, many numerical models have to be created and solved in the process of back analysis each time. Finally, the statistical learning method, with an artificial intelligent algorithm as the kernel, can well address this issue and improve the computational efficiency. With the rapid development of big data science in recent years, intelligent algorithms, including the artificial neural network (ANN), support vector machine (SVM), Gaussian process (GP), and extreme learning machine (ELM), have been successfully applied in geotechnical engineering (Zhou et al. 2016; Xue and Xiao 2017; Xue et al. 2020; Zhang et al. 2020a, b). These intelligent data-driven models can map any nonlinear relationship without prior assumptions relating to the data (Feng et al. 2004) and may become a substitute for numerical analysis through sample training. Thus, the problem of numerical back analysis can be transformed into an optimization problem without the excessive computational burden.

In earlier studies, when performing displacement-based back analysis, researchers often neglected two main points:

- The first is displacement loss. In a rock tunnel, the displacement monitors are generally assembled after the completion of the first lining as the excavation work continues. Therefore, there would always be a distance d between the monitoring section and the tunnel face, as depicted in Fig. 1a. The rock displacement that occurs before the installation of instruments is not recorded. The monitoring curve is only a part of the total displacement curve (shown with a solid line in Fig. 1b), and the rest of the curve is termed the displacement loss (represented with the dashed line in Fig. 1b), which can be subdivided into three parts: the displacement occurs before the excavation of the tunnel face, the displacement occurs after the excavation and before the construction of first lining, and the displacement occurs after the first lining construction and before the installation of monitors. However, in numerical simulations, displacement can be recorded as soon as the rock excavation. In the process of displacement-based back analysis, if simulation displacement is calculated to approach the monitoring displacement without subtracting the displacement loss, a large negative effect would be caused on the precision of prediction. For several years, displacement loss has been considered based on the load release coefficient (Yang et al. 1983; Lu et al. 2014; Gao and Ge 2016), which is uncertain because it is determined by engineering experience. Recently, some researchers have noticed this issue (Zhang et al. 2020b), and more effective methods are in need to be proposed to consider displacement loss.
- The second is the space effect. When a tunnel is excavated, the displacement of the rock varies with the excavation process. This space effect is sufficiently reflected in the displacement curve. However, in many back analysis studies (Song et al. 2015; Wu et al. 2019; Xu and Ni 2019), researchers often have neglected the process of displacement variation and have used the final value of displacement, which would affect the accuracy and applicability of back analysis method. Reasons are that the vault settlement or horizontal convergence may be the same for two tunnel excavation cases, whereas the displacement curves cannot be identical because of different rock categories, initial stress states, and construction methods. Therefore, it is necessary to consider the space effect when performing displacement-based back analysis.

This paper proposes a displacement-based back analysis approach that considers the displacement loss and space effect, to predict the parameters of surrounding rocks during tunnel excavation. The core algorithm is referred to as PSO-ELM-PSO, in which the ELM model optimized by the PSO algorithm works as a substitution for the numerical analysis, and the PSO algorithm is utilized again to search for the optimal rock parameters. The process and detailed considerations of the proposed method are introduced in the "Methodology" section. A case study for validating the method and investigating the impact of the monitoring parameters on the accuracy of the algorithm is presented in the "Case study" section. In the "Engineering application" section, the application of the method to the excavation of a tunnel in Shenzhen, China, is described. Thereafter, the PSO-ELM-PSO and PSO-ELM algorithms are compared, and the limitations and prospects of the proposed method are discussed in the "Discussion"

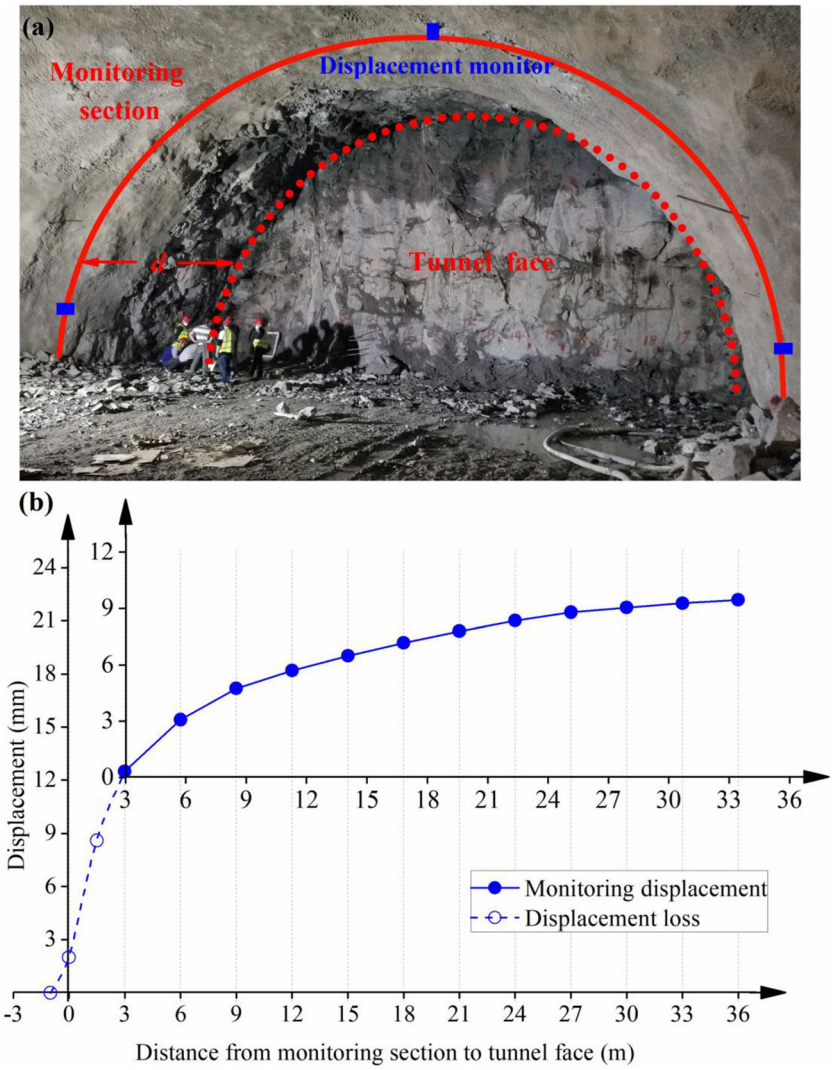

Fig. 1 **a** Positions of initial monitoring section and tunnel face in practical excavation. **b** Profiles of monitoring displacement and displacement loss

section. Finally, the principal conclusions of this study are summarized in the "Conclusions" section. The primary novelty of this study has two aspects. (1) An integrated algorithm named PSO-ELM-PSO is applied to back analyze rock parameters in the tunnel construction, in which the displacement loss and space effect are both considered. (2) The variation law of prediction error is revealed on the selection of the rock parameters and the change of the monitoring parameters. Measures are also provided to improve the quality of training samples and the precision of the algorithm.

Methodology

The proposed displacement-based back analysis method comprises three key parts:

- The selection of the output parameters, in which the displacement loss and space effect are considered, is described in the "Consideration of displacement loss" and "Consideration of space effect" sections.
- The selection of the input parameters, which is supported by the sensitivity analysis, is presented in the "Establishment of training set" section.
- The development of the back analysis algorithm, which combines PSO and an ELM, is introduced in the "Process of back analysis algorithm" section.

Consideration of displacement loss

As discussed above, displacement loss cannot be avoided in field monitoring, and it is relevant to the initial monitoring time or distance. In numerical simulations, the displacement values are generally considered functions of the computation time, and the resultant curve is the time–displacement curve. Because the actual construction time is different from the computation time and the initial monitoring time is difficult

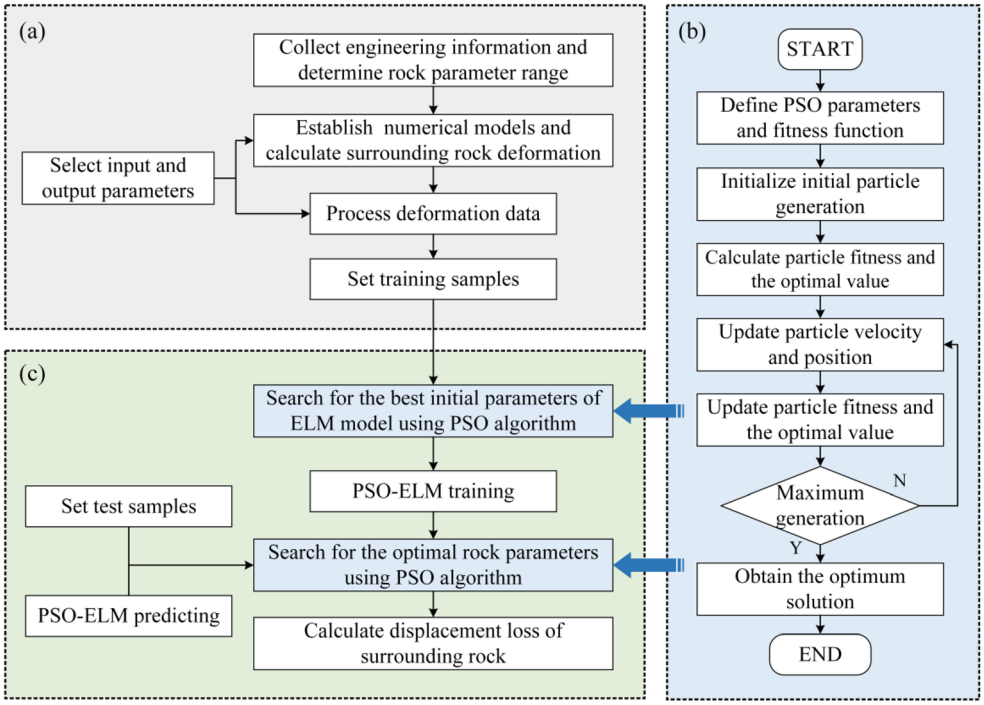

Fig. 2 Flowchart of proposed back analysis method: processes of (a) setting train samples, (b) PSO algorithm, and (c) PSO-ELM-PSO algorithm

to determine from the time–displacement curve, it is hard to correlate the monitoring curve with the simulation curve and perform displacement-based back analysis. Nevertheless, the distance between the monitoring section and the tunnel face can easily be measured, and the initial monitoring distance remains stable (usually equal to the length of one construction footage) for a specific tunnel section.

In this study, both the simulation and monitoring displacements were recorded according to the monitoring distance. The steps of a simple procedure used to predict the rock parameters and displacement loss are listed as follows: (1) conduct numerical analyses with different rock parameters, (2) select parts of the total distance–displacement curves as the simulation monitoring curves, (3) map the simulation monitoring curves to the rock parameters, (4) predict the actual rock parameters based on the actual monitoring curve, (5) compute the total displacement curve using the predicted rock parameters, and (6) predict the actual displacement loss. It should be noted that the displacement loss is considered the summation. The three parts of displacement loss are not studied in detail in this research.

Consideration of space effect

As mentioned in the "Introduction," most previous studies have performed back analysis based on the final value of the monitoring displacement, regardless of the variation process. In the present study, the space effect is considered by introducing parameters representing the rock deformation process, together with the final values of displacement, as the output parameters of the algorithm. That is, the monitoring displacement curve is fitted with an empirical equation, and the fitting parameters are considered the process-representing parameters of rock deformation. This study employs the equation in the natural logarithmic form (Zhang et al. 2009):

$$U = a + b \times \log(1 + d) \tag{1}$$

where U is the rock displacement, a and b are the fitting parameters, and d is the monitoring distance.

In addition, the displacement curves for different monitoring positions in the tunnel cross-section are different, resulting in many sets of fitting parameters. To reduce the number of calculations, displacement values, normalized using Eq. (2), at one typical position (e.g., the tunnel vault) are chosen to calculate the process-representing parameters (a and b in Eq. (1)). The final values of vault settlement, horizontal convergence, and so on are the result-representing parameters. These two types of parameters constitute the output parameters of the algorithm.

$$\overline{u_i} = \left(|u_i| - |u|_{\min}\right) / \left(|u|_{\max} - |u|_{\min}\right) \tag{2}$$

where u_i is a series of displacement values, $\overline{u_i}$ is the normalized displacement values, i is the series number, and $|u|_{\max}$ and $|u|_{\min}$ are the maximum and minimum of the absolute displacement values.

Establishment of training set

Before initiating the primary algorithm, the training samples should be set as the objects for machine learning; the

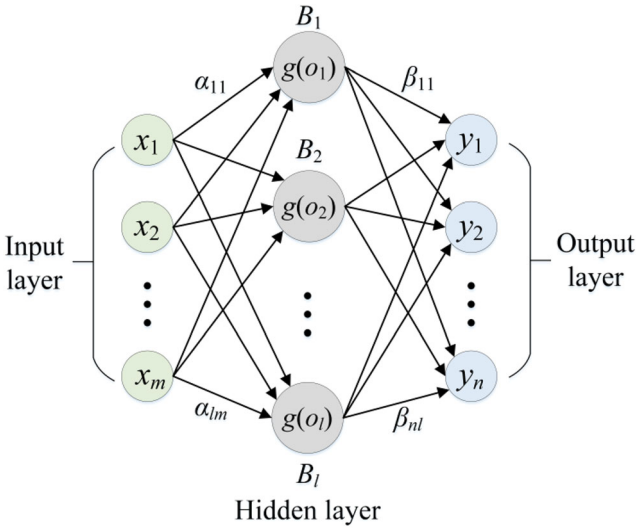

Fig. 3 Structure of ELM algorithm

procedure is presented in Fig. 2(a). To ensure the quality of training samples and the accuracy of the algorithm, a relatively strong correlation is required between the input and output parameters. Sensitivity analysis (Sharifzadeh et al. 2013) can be performed to identify the input parameters most relevant to output parameters.

In this study, the outputs of the system are the displacement parameters (vault settlement, horizontal convergence, fitting parameters of displacement curve, and so on), which are affected by numerous factors (geostatic stress, rock mechanical parameters, and so on). These n factors, which can also be seen as potential inputs, are written as $\{\alpha_1, \alpha_2, \alpha_3, \ldots, \alpha_n\}$, and the relevant output parameters are defined as $f\{\alpha_1, \alpha_2, \alpha_3, \ldots, \alpha_n\}$. During the sensitivity analysis, the parameter α_i varies within a specific range ($\pm\Delta\alpha_i$) whereas all the other parameters remain constant. The sensitivity of α_i can be calculated using the sensitivity function, as follows:

$$S(\alpha_i) = \sum_{j=1}^{k} S_j = \sum_{j=1}^{k} \left| \frac{f(\alpha_i + \Delta\alpha_i) - f(\alpha_i - \Delta\alpha_i)}{f(\alpha_i)} \right| / \left(\frac{2\Delta\alpha_i}{\alpha_i} \right) \quad (3)$$

where $S(\alpha_i)$ is the sensitivity of α_i and k is the number of output parameters.

After the sensitivity analysis, parameters with large sensitivities would be selected as the inputs. Thereafter, numerical models with different sets of selected input parameters can be built and calculated. Subsequently, the computational deformation data would be recorded and processed as the outputs. By integrating the values of the input and output parameters, the training set could finally be established. Detailed procedures of setting the training samples for a specific case could be seen in the "Model settings and operation" section.

Process of back analysis algorithm

Particle swarm optimization

Inspired by the behavior of bird foraging, Eberhart and Kennedy (1995) proposed an innovative global optimization algorithm named particle swarm optimization. The PSO algorithm is initialized with a "swarm" of random particles. Each particle indicates a potential solution to the problem, and has three characteristic indices: position, velocity, and fitness value. During optimization, particles tend to move toward their individual best positions (P_{best}) and the global best position (G_{best}), based on the velocity and distance from the best positions (Jahed Armaghani et al. 2020). The values of P_{best} and G_{best} are determined using the particle fitness value, which is calculated using the predefined fitness function. In this study, the fitness function of PSO can be expressed as

$$fitness = \sum_{i=1}^{n} \sum_{j=1}^{m} \left(T_{ij} - T'_{ij} \right)^2 / mn \quad (4)$$

where m and n are the numbers of samples and output parameters, respectively, and T and T' denote the actual and simulation values, respectively. The process of PSO can be seen in Fig. 2(b). In every iteration, the particle velocity and position are updated using the following equations:

$$\begin{cases} X_i^{m+1} = V_i^{m+1} + X_i^m \\ V_i^{m+1} = \omega^m \times V_i^{m+1} + c_1 \times r_1 \times \left(P_{\text{best}}^m - X_i^m \right) + c_2 \times r_2 \times \left(G_{\text{best}}^m - X_i^m \right) \end{cases} \quad (5)$$

where m is the current iteration number; V_i and X_i are the

Table 1 Comparison of the results obtained with different machine learning methods

Method	Key parameters	Mean square error	Computing time (s)
Back-propagation (BP)	Two hidden layers with 5 nodes of each	1.3990	1.6244
Radial basis function (RBF)	Spread = 0.8	0.3060	0.7160
Support vector machine (SVM)	Default in the Matlab Toolbox LIBSVM	0.0141	12.7372
ELM	The input weights and hidden biases are random.	1.2882	0.1702
PSO-ELM	The input weights and hidden biases are optimized by PSO. Number of iteration = 100 Size of population = 50	0.0022	1.8968

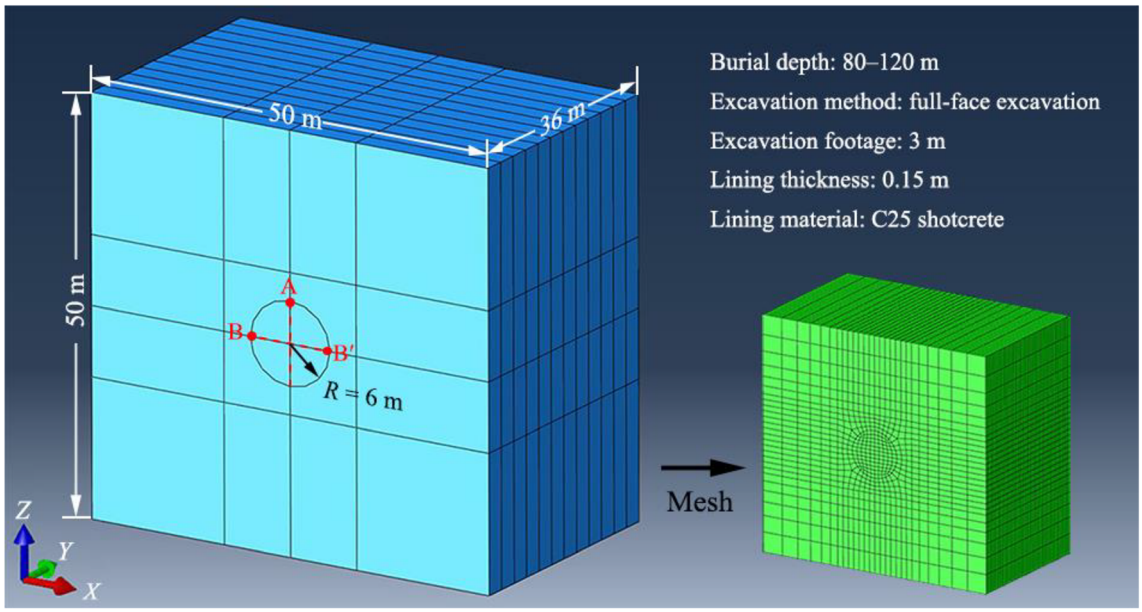

Fig. 4 Numerical model of deep buried circular tunnel

velocity and position vectors, respectively, of particle i; c_1 and c_2 represent the acceleration constants and are set as 1.2 in this study; r_1 and r_2 are two random numbers uniformly distributed in [0 1]; and ω is the inertia weight factor with a linear decreasing form and can be calculated as follows:

$$\omega^m = \omega_{\text{start}} - (\omega_{\text{start}} - \omega_{\text{end}}) \times m/m_{\max} \tag{6}$$

where $m_{\max}$ is the maximum of the iteration number; ω_{start} and ω_{end} correspond to the initial and final inertia weights and are usually set as 0.4 and 0.9, respectively (Xue and Xiao 2017; Zhang et al. 2020a, b).

Extreme learning machine

The extreme learning machine, proposed by Huang et al. (2004), is a modification of the feedforward neural network with a single hidden layer. It features a high learning speed and exhibits remarkable generalization performance, and has been widely applied in recent years (Song et al. 2015; Xue et al. 2020).

The typical structure of the ELM model, composed of the input layer (with m nodes), output layer (with n nodes), and hidden layer (with l nodes), can be seen in Fig. 3. We assume that there are Q different training samples (X_i, Y_i) $(i = 1, 2, \ldots, Q)$ for the ELM model; $X_i = [x_1, x_2, \ldots, x_m]^{\mathrm{T}}$ and $Y_i = [y_1, y_2, \ldots, y_n]^{\mathrm{T}}$ are the input and output parameters. $\alpha_{l\times m}$ and $\beta_{n\times l}$ are the connection weights from the input layer to the hidden layer and the hidden layer to the output layer, respectively, and $B = [b_1, b_2, \ldots, b_l]^{\mathrm{T}}$ is the bias of the hidden layer. Employing the active function $g(x)$, the goal of the ELM training can be expressed as

$$\sum_{i=1}^{Q} \| Y_i - \beta_{n\times l} g(\alpha_{l\times m} X_i + B_{l\times 1}) \| \to 0 \tag{7}$$

The input connection weight $\alpha_{l\times m}$ and hidden layer bias B are assigned randomly, and the output connection weight $\beta_{n\times l}$ can be calculated using the least squares method (Huang et al. 2006).

Generally, in modeling data using ELM, the standard training algorithm includes three steps (Song et al. 2015): (1) determine the node number of the hidden layer and set the input connection weight $\alpha_{l\times m}$ and hidden layer bias B, (2) select an infinite differentiable function as the activation function and

Table 2 Parameter settings of rock and lining for the deep buried circular tunnel

Rock							Lining		
γ (kN/m^3)	E (GPa)	μ	c (MPa)	φ (°)	λ_x	λ_y	γ (kN/m^3)	E (GPa)	μ
25	1–5	0.3–0.35	0.3–0.5	25–35	1.1–1.5	0.7–0.9	23	26	0.2

γ is the unit weight; E is the elastic modulus; μ is the Poisson's ratio; c is the cohesive force; φ is the internal friction angle; λ_x is the lateral pressure coefficient in x-direction, which is perpendicular to tunnel axis; λ_y is the lateral pressure coefficient in y-direction, which is parallel to tunnel axis

Table 3 The sensitivity of rock parameters

	E	μ	c	φ	H	λ_x	λ_y
Sensitivity value	1.09	0.59	0.18	0.55	1.82	2.27	0.32

γ is the unit weight; E is the elastic modulus. μ is the Poisson's ratio; c is the cohesive force; φ is the internal friction angle; H is the burial depth; λ_x is the lateral pressure coefficient in x-direction, which is perpendicular to tunnel axis; λ_y is the lateral pressure coefficient in y-direction, which is parallel to tunnel axis

calculate the output array of the hidden layer, and (3) calculate the output connection weight $\beta_{n\times l}$. However, recent literature has revealed that the solution models of basic ELM might get trapped in local minima owing to the stochastic initialization of the input weights and hidden biases (Cao et al. 2012). Optimization algorithms, e.g., the cuckoo search algorithm (Mohapatra et al. 2015) and firefly algorithm (Satapathy et al. 2017), can be used to improve the generalization capacity of the ELM.

PSO-ELM-PSO

Table 1 shows the results obtained with several typical machine learning methods to fit the nonlinear function $y = x + x^2 + 2\sin(\pi x), \quad x \in [-5, 5]$. Two hundred data samples uniformly distributed in the domain are selected as the learning set, and 10 data samples are randomly chosen as the testing set. The performance of the methods are evaluated by the mean square error of the testing data and the computing time. It can be seen that the PSO-ELM method features high precision and relatively short computing time.

In this study, the process of the integrated use of PSO and ELM is presented in Fig. 2(c). First, PSO is employed to optimize the input weights and hidden biases of the ELM. Subsequently, the PSO-ELM model is trained to substitute for the numerical analysis of tunnel excavation. After the preparation of the testing samples, PSO is again used to determine the best rock parameters, based on which the displacement variation closest to the monitoring curve can be calculated. Finally, numerical models are solved using the optimal rock parameters, and the displacement loss of the surrounding rock can be predicted.

In addition, a slight fluctuation has been observed in the results of PSO-ELM-PSO owing to different sets of weights and thresholds in every searching process. To avoid the accidental error, the principal program is run 20 times, and the average value is taken as the final result. This has been proven to be a feasible way to improve the precision of the algorithm (Zhang et al. 2020a, b).

Table 4 Orthogonal design levels of the rock parameters

Parameter	Level				
	1	2	3	4	5
E (GPa)	1.0	2.0	3.0	4.0	5.0
μ	0.31	0.32	0.33	0.34	0.35
H (10^2 m)	0.8	0.9	1	1.1	1.2
λ_x	1.1	1.2	1.3	1.4	1.5

E is the elastic modulus; μ is the Poisson's ratio; H is the burial depth; λ_x is the lateral pressure coefficient in x-direction, which is perpendicular to tunnel axis

Case study

To verify the performance of the proposed back analysis method, simulations were conducted for the excavation of a deep buried tunnel.

- The details of the numerical models and settings for the algorithm are presented in the "Model settings and operation" section.
- The results of the prediction, along with the error analysis, are presented in the "Results of prediction" section.
- Further details regarding the impact of the rock parameters and monitoring parameters are discussed in the "Analysis of rock parameters" and "Analysis of monitoring parameters" sections.

Model settings and operation

A three-dimensional model (Fig. 4) was established using the finite element software ABAQUS 6.13 for predicting the parameters of rock mass in a tunnel under construction. This circular tunnel, with a diameter of 12 m, was buried 80–120 m beneath the ground and fully excavated. The area of the surrounding rock in the xz plane was 50 m × 50 m. The total excavation length was 36 m in the model and the excavation footage was 3 m. The horizontal displacement was constrained at the left, right, front, and back boundaries, and the vertical displacement was constrained at the bottom boundary of the model. Pressure was applied on the top boundary to simulate vertical load of rock. The widely used Mohr–Coulomb model was adopted as the constitutive model, while the elastic model was adopted for the tunnel lining, which was composed of C25 shotcrete. The values of the rock parameters that varied within certain ranges are listed in Table 2.

According to the procedures described in the "Methodology" section and presented in Fig. 2, the following steps were adopted to execute the back analysis algorithm.

Table 5 Prediction results and relative errors obtained using PSO-ELM-PSO method for different testing samples.

Testing sample		E (GPa)	μ	λ_x	H (10^2 m)
Sample 1	Predefined value	2.60	0.32	1.24	1.05
	Back analysis value	2.677	0.326	1.246	1.076
	Relative error	2.96%	1.88%	0.48%	2.48%
	Average	1.95%			
Sample 2	Predefined value	3.40	0.33	1.32	0.95
	Back analysis value	3.275	0.326	1.339	0.933
	Relative error	3.68%	1.21%	1.44%	1.79%
	Average	2.03%			
Sample 3	Predefined value	4.50	0.34	1.46	1.08
	Back analysis value	4.605	0.335	1.451	1.109
	Relative error	2.33%	1.47%	0.62%	2.69%
	Average	1.78%			

E is the elastic modulus; μ is the Poisson's ratio; H is the burial depth; λ_x is the lateral pressure coefficient in x-direction, which is perpendicular to tunnel axis

STEP 1: The final values of vault settlement (U_A) and horizontal convergence ($U_{BB'}$), along with the fitting parameters (a, b) calculated using Eqs. (1) and (2), were selected as the output parameters of the algorithm. The monitoring positions are marked as A, B, and B′ in Fig. 4.

STEP 2: The sensitivity analysis was conducted using Eq. (3); the sensitivity of the rock parameters can be determined from Table 3. Four parameters with relatively large sensitivities (elasticity modulus, Poisson's ratio, burial depth, and lateral pressure coefficient in the x-direction) were chosen as the input parameters. The other parameters were set constant in the numerical models.

STEP 3: Based on the ranges of the rock parameters presented in Table 2, each selected input parameter was divided into five levels, as listed in Table 4. By employing the orthogonal table of six factors and five levels, 25 numerical models were built and calculated. The inputs were obtained by the orthogonal design table, and the outputs were acquired from the computational displacement data of the 25 numerical models. By integrating all the values of the input and output parameters, the training set was established.

STEP 4: Six numerical models with the predefined rock parameters within their ranges were calculated and regarded as the actual situations. Referring to common engineering practice, the rock displacements began to be recorded after the construction of the first lining. The values of input and output parameters were combined as the testing set.

STEP 5: Based on the training samples, the PSO-ELM-PSO algorithm, programmed in MATLAB R2013a, was applied, and the rock parameters of the three models were predicted.

STEP 6: Numerical models were solved using the predicted rock parameters, and the total displacement curves and the displacement loss were finally computed.

Results of prediction

Table 5 presents the results of the prediction and the relative errors for three of the testing samples in details. The relative errors of all the parameters are acceptable, of which the maximum is below 5%. Relatively speaking, the errors of the parameters with large sensitivities are small. For example, the sensitivity of the lateral pressure coefficient in the x-direction (λ_x) is 2.27, which is the peak, and the error can be as low as 0.48%, which is the lowest among all the results. Nevertheless, the Poisson's ratio (μ) seems to be the exception. Although the sensitivity of the Poisson's ratio (μ) is only 0.59, the relative error is slight. This is because the variation range of μ is small, resulting in a relatively accurate prediction. The comparisons between the simulated and monitoring displacement curves are presented in Fig. 5. It can be seen that all the simulation curves agree well with the monitoring curves. The displacement loss occurring before the construction of the lining accounts for 20–30% of the total displacement, which is in line with engineering experiences and the results of previous studies (Zhang et al. 2009). This analysis of the results of the predictions indicates that the proposed back

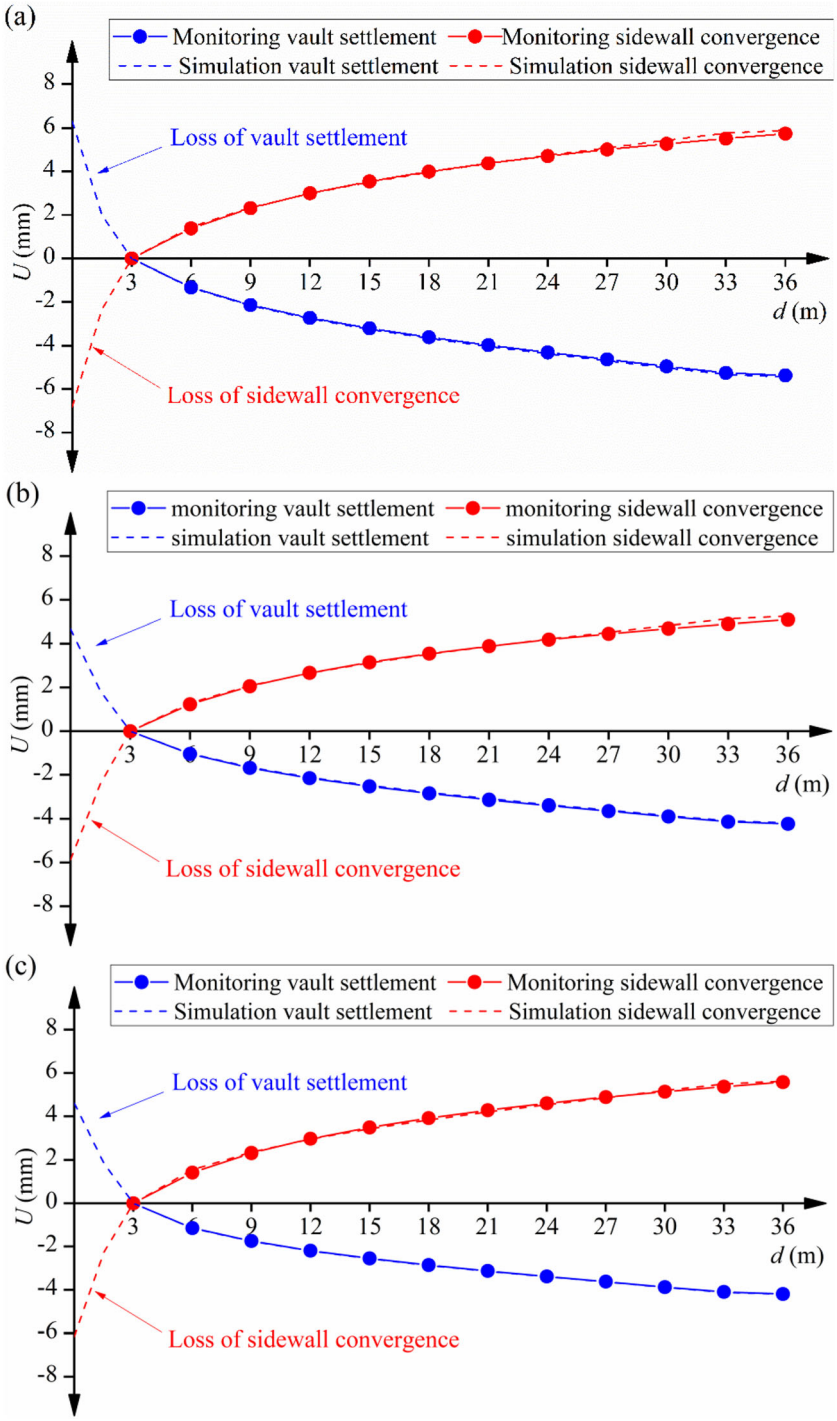

Fig. 5 Comparisons of monitoring and simulating displacement curves for **a** sample 1, **b** sample 2, and **c** sample 3

analysis method can provide reliable results and is feasible for engineering applications.

The prediction results with and without considering displacement loss and space effect can be seen in Table 6. To avoid the influence caused by the difference of testing samples, the relative errors of all the testing samples for the four rock parameters are averaged out, and the average error of the four rock parameters is also calculated. When the displacement loss and space effect are both considered in back analysis, the relative errors of the four rock parameters are low, and the average error is 2.76%. In the case without considering the space effect, the relative error in elastic modulus increases threefold, and the average error rises to 6.59%. When displacement loss is not considered, the errors of all the

Table 6 Prediction errors obtained using PSO-ELM-PSO method with and without considering displacement loss and space effect

Considering factors		E (GPa)	μ	λ_x	H (10^2 m)
Displacement loss and space effect	Relative error	4.96%	2.16%	1.13%	2.79%
	Average	2.76%			
Displacement loss	Relative error	16.21%	2.39%	1.24%	6.53%
	Average	6.59%			
Space effect	Relative error	28.16%	4.39%	5.59%	12.7%
	Average	12.71%			

E is the elastic modulus; μ is the Poisson's ratio; H is the burial depth; λ_x is the lateral pressure coefficient in x-direction, which is perpendicular to tunnel axis

parameters increase significantly, and the average error is 4.6 times of that in the original case. Therefore, it is important and necessary to consider the displacement loss and space effect in back analysis of rock parameters.

Analysis of rock parameters

In previous literature on displacement-based back analysis, some researchers selected elasticity modulus and Poisson's ratio as the target parameters, while others selected three or more rock parameters based on different considerations. In this study, four rock parameters with relatively large sensitivities were chosen as the inputs. To study the effects of rock parameter selection, the simulations were performed as follows:

- Case 1: Two rock parameters (elasticity modulus and Poisson's ratio) were selected as the input parameters.
- Case 2: Four parameters (elasticity modulus, Poisson's ratio, burial depth, and lateral pressure coefficient in the x-direction) were selected as the input parameters.
- Case 3: Six parameters (elasticity modulus, Poisson's ratio, burial depth, lateral pressure coefficient in the x-direction, cohesive force, and internal friction angle) were selected as the output parameters.

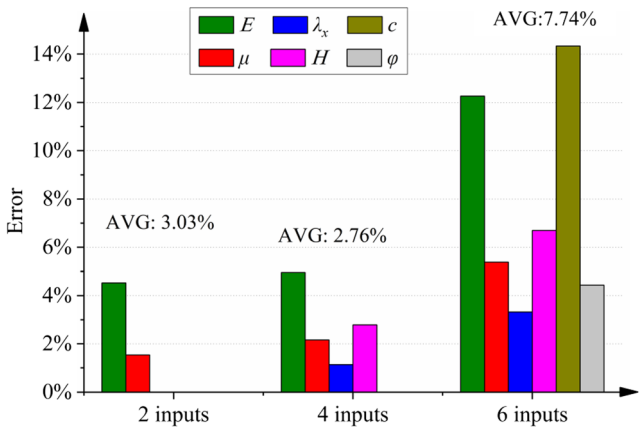

Fig. 6 Error variations in rock parameters for different inputs

The results of the prediction are provided in Fig. 6. The errors of parameters in the case of 2 inputs are close to those in the case of 4 inputs. However, when input number increases to 6, a large growth is witnessed in errors of all the parameters. The average error rises to 7.74%, nearly three times of that in the case of 4 inputs. It can be explained that the sensitivity value is relatively low for cohesive force and internal friction angle (Table 3). Introducing these two parameters to the inputs would reduce the quality of training samples, causing the decrease of prediction accuracy. Therefore, when establishing the training set, it is suggested to choose parameters with high correlations as the inputs and outputs.

Analysis of monitoring parameters

During tunnel construction, some monitoring parameters, such as monitoring lines, initial monitoring distance, and monitoring frequency, may change because of different rock grades, construction programming, or some other factors. To test the adaptability of the proposed method to variations in the monitoring parameters, researches on monitoring parameters were performed as in Fig. 7.

Effect of monitoring lines

When studying the effects of monitoring lines, the simulations were performed as follows:

- Case 1: Lines A and BB′ were monitored. Two parameters (U_A, $U_{BB'}$) and four parameters (U_A, $U_{BB'}$, a, b) were selected as the output parameters.
- Case 2: Lines A, BB′, and AB (equal to line AB′) were monitored. Five parameters (U_A, $U_{BB'}$, U_{AB}, a, b) were selected as the output parameters.
- Case 3: Lines A, BB′, AB (equal to line AB′), and CC′ were monitored. Six parameters (U_A, $U_{BB'}$, U_{AB}, $U_{CC'}$, a, b) were selected as the output parameters.

The results of the prediction are provided in Fig. 8a. In the different cases of monitoring lines, the errors in λ_x remain low,

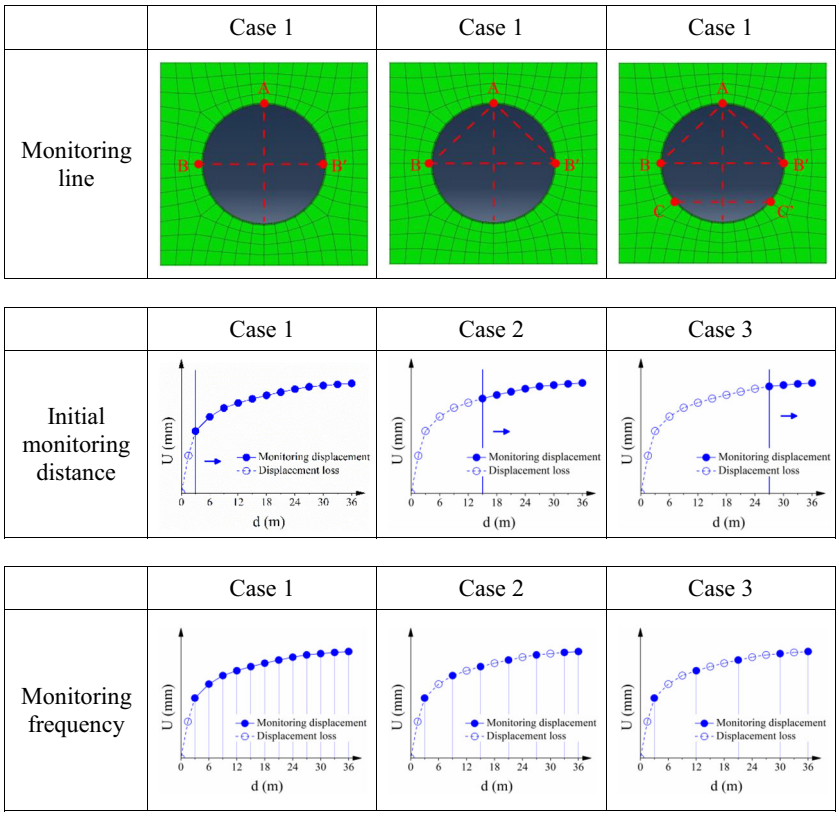

Fig. 7 Simulation arrangement for analysis of monitoring parameters

whereas those in E fluctuate sharply. This may be attributed to the relatively low sensitivity and a wide range of variation in E. With the increase of monitoring lines, the average error also grows. It is because the increase of monitoring lines does not mean the improvement of the quality of the training samples. In fact, adding displacement data with low correlation with rock parameters to the training set would reduce the prediction accuracy. As a consequence, it is preferred to use displacement data at typical positions (vault settlement and horizontal convergence) when performing displacement-based back analysis.

Effect of initial monitoring distance

In studying the effects of the initial monitoring distance, the simulations were arranged as follows:

- Case 1: The distance between the initial monitoring section and tunnel face was 3 m.
- Case 2: The distance between the initial monitoring section and tunnel face was 15 m.
- Case 3: The distance between the initial monitoring section and tunnel face was 27 m.

The results of the prediction are provided in Fig. 8b. The relative errors vary a little with the changes in the initial monitoring distance. It can be inferred that the changes in the initial monitoring distance result in minor fluctuations in the results of the prediction, and that a certain delay in monitoring would not affect the accuracy of the algorithm. It should be noted that with the increase of the initial monitoring distance, the error in λ_x increases and that in H decreases. In the case that the initial monitoring distance is 27 m, the error in λ_x is close to that in E, and the error in H becomes the lowest. Possible reasons are given that the sensitivity value of rock parameter may change for different parts of displacement curve. The displacement variations are not so sensitive to the changes of E when the rock deformation becomes gradually stable, causing the relatively larger prediction error in E.

Effect of monitoring frequency

In studying the effects of monitoring frequency, the simulations were performed as follows:

- Case 1: Monitoring data were recorded every 3 m of excavation length.
- Case 2: Monitoring data were recorded every 6 m of excavation length.
- Case 3: Monitoring data were recorded every 9 m of excavation length.

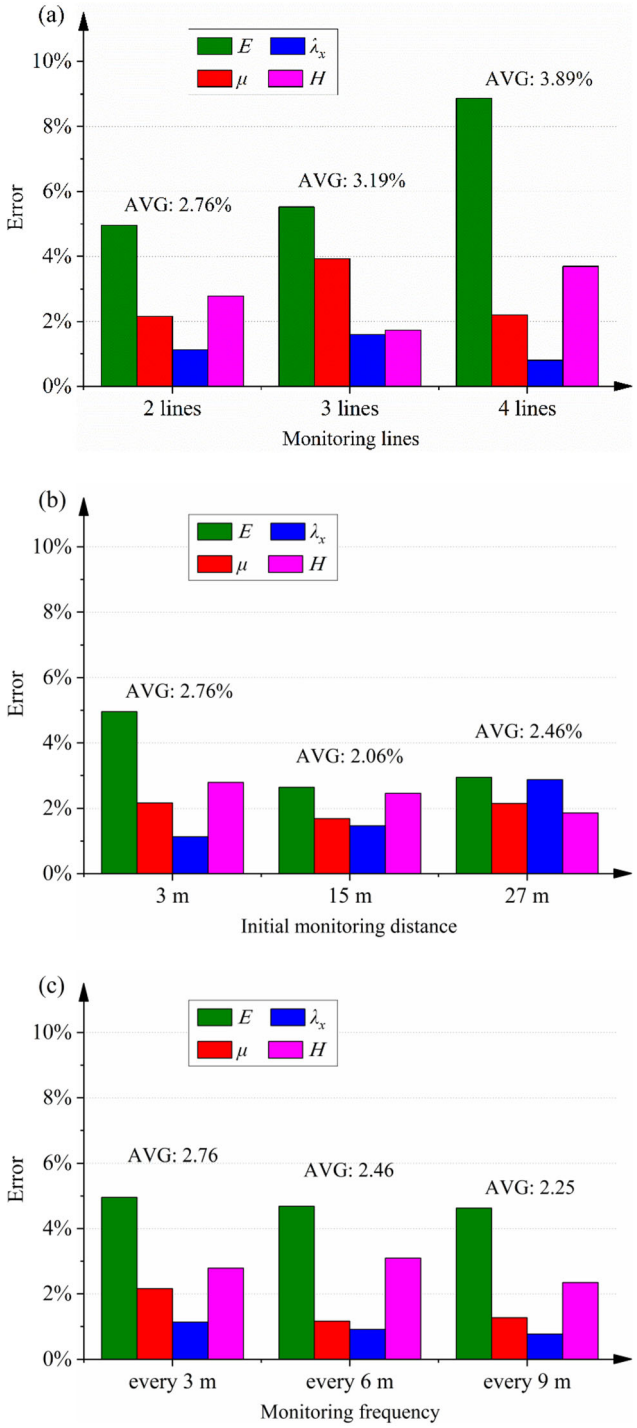

Fig. 8 Error variations in rock parameters for **a** monitoring line, **b** initial monitoring distance, and **c** monitoring frequency

The results of the prediction are listed in Fig. 8c. For different monitoring frequencies, the order sorted by relative error of the rock parameter is unchanged. Although no apparent rule is found in the error variations of the rock parameters, the average error declines with the decrease in the monitoring frequency. It can be inferred that a low monitoring frequency, or generally, selecting typical monitoring values to set the training samples, would assist in the improvement of the accuracy of the algorithm.

Engineering application

The Jigongshan Mountain Tunnel, part of the Banyin Expressway connecting the Luohu District and the Longgang District in Shenzhen, China, is designed to pass underneath the Xiaping Municipal Solid Waste (MSW) Landfill (Feng et al. 2020). Figure 9a depicts the position and route of the tunnel. It is a separated tunnel with a length of 4.6 km and a six-lane expressway in both directions. The particular form of the three-center circle was adopted for the inner contour of the tunnel owing to its good mechanical performance and the tunnel net width was approximately 15 m. A new Austrian method and the benching tunneling method were employed for tunnel construction, and the vault settlement and horizontal convergence were monitored during tunnel excavation (Fig. 9b). In the preliminary geological investigation, the geostress was measured in the geological borehole SD-X24 using the hydro fracturing method. The position of the borehole is marked in Fig. 9a, and the results are presented in Table 7. Considering the orientation of the tunnel axis near SD-X24, the lateral pressure coefficient in the direction of the tunnel cross-section was calculated to be approximately 1.8.

The proposed back analysis method was applied to the LK2+820 tunnel section, which is near the borehole SD-X24, to estimate the surrounding rock parameters and displacement loss. The numerical model is depicted in Fig. 10, and the parameter ranges are listed in Table 8. Because the burial depth of LK2+820 was ascertained to be 200 m via the preliminary geological investigation, three other parameters (elasticity modulus, Poisson's ratio, and lateral pressure coefficient in the *x*-direction) were chosen as the input parameters, based on the sensitivity analysis. All the training samples were set following orthogonal design and learned by the proposed algorithm.

The total displacement curve and rock parameters were predicted based on the monitoring data recorded during the construction process. The monitoring and simulation displacement curves are exhibited in Fig. 11. Although the construction footage varies within 2–4 m in the practical excavation process, the simulation curves could still match the monitoring data well. Further, the displacement loss occurring before the construction of the lining accounts for 30% of the total displacement. The values of the elasticity modulus, Poisson's ratio, and lateral pressure coefficient were estimated to be 9.38 GPa, 0.266, and 1.83, respectively. The predicted lateral pressure coefficient is in accordance with the results of the geostress measurement, indicating that the proposed method

Table 7 Results of the geostress measurement using hydro fracturing method for borehole SD-X24

Testing section	Depth (m)	σ_H (MPa)	σ_h (MPa)	σ_V (MPa)	λ_H	Orientation of σ_H
1	97.7	2.0	1.9	2.6	0.8	/
2	121.6	2.4	2.1	3.3	0.7	/
3	147.6	3.6	3.1	4.0	0.9	/
4	159.8	8.8	5.4	4.3	2.1	NE86°
5	174.2	10.2	6.6	4.7	2.2	/
6	183.7	10.0	6.4	5.0	2.0	/
7	191.0	9.5	5.8	5.2	1.8	/
8	198.1	10.3	6.4	5.3	1.9	/
9	201.1	10.7	6.8	5.4	2.0	/
10	203.9	10.6	6.9	5.5	1.9	NE61°

σ_H is the horizontal major principal stress; σ_h is the horizontal minor principal stress; σ_V is the vertical principal stress; λ_H is the lateral pressure coefficient in the direction of the horizontal major principal stress, which is calculated as σ_H/σ_V

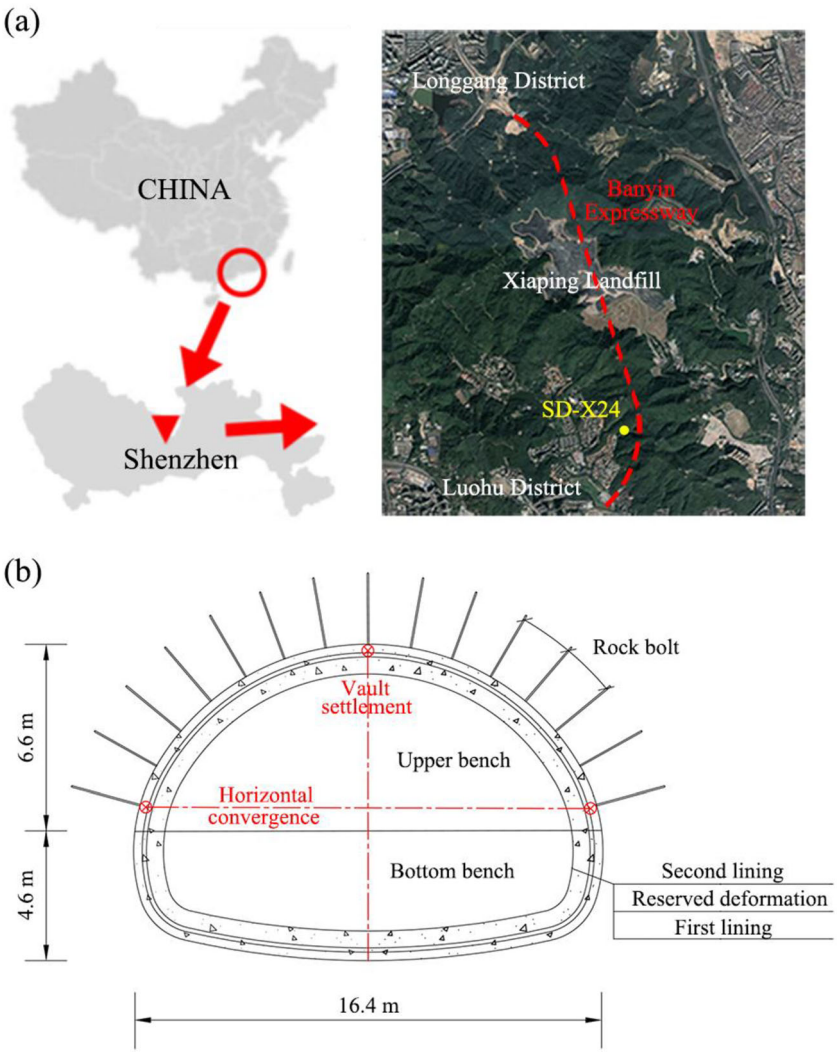

Fig. 9 **a** Location and route of tunnel in case study. **b** Tunnel cross-section of LK2+820 and monitoring lines

Table 8 Parameter settings of rock and support system for the tunnel section of LK2+820

Rock						
γ (kN/m^3)	E (GPa)	μ	c (MPa)	φ (°)	λ_x	λ_y
25	8-12	0.26–0.30	0.3–0.5	25–35	1.6–2.0	1.1–1.3
Lining			**Rock bolt**			
γ (kN/m^3)	E (GPa)	μ	γ (kN/m^3)	E (GPa)	μ	Length (m)
23	26	0.2	78	200	0.25	1.5

γ is the unit weight; E is the elastic modulus; μ is the Poisson's ratio; c is the cohesive force; φ is the internal friction angle; λ_x is the lateral pressure coefficient in x-direction, which is perpendicular to tunnel axis; λ_y is the lateral pressure coefficient in y-direction, which is parallel to tunnel axis

provides a suitable alternative approach for estimating ground stress and, thus, can be studied further.

Discussion

Comparison with PSO-ELM method

In the PSO-ELM-PSO method, the PSO-ELM algorithm was employed as a substitution for the numerical analysis, and the PSO algorithm was used to search for the best solution. Subsequently, in the PSO-ELM model proposed herein, the parameters to be predicted were set as the input parameters, and the known parameters were set as the outputs. However, several researchers have considered the opposite case (Song et al. 2015; Gao and Ge 2016; Zhang et al. 2017). Thus, the target parameters can be predicted as long as the monitoring data are inputted. In this section, we present a comparison between the two abovementioned methods based on the data provided in the case study.

The prediction results of PSO-ELM are presented in Table 9. The relative errors for some parameters are small, whereas others are significantly higher compared to those for PSO-ELM-PSO, as presented in Table 5. Figure 12 presents the convergence of PSO-ELM-PSO and PSO-ELM in the sample-learning procedure. It can be seen that the fitness value of PSO-ELM-PSO is much lower, and the convergence rate of PSO-ELM-PSO is significantly faster than that of PSO-ELM. This is because when the training samples of PSO-ELM-PSO are arranged, the input rock parameters can be set based on the orthogonal design. Moreover, the input parameters of PSO-ELM are displacement values, which are calculated using numerical models and are difficult to arrange. Therefore, the quality of the PSO-ELM training samples is worse, resulting in a higher fitness value and higher errors in prediction.

Limitations and prospects

Based on the comparison presented in the "Comparison with PSO-ELM method" section, it can be inferred that

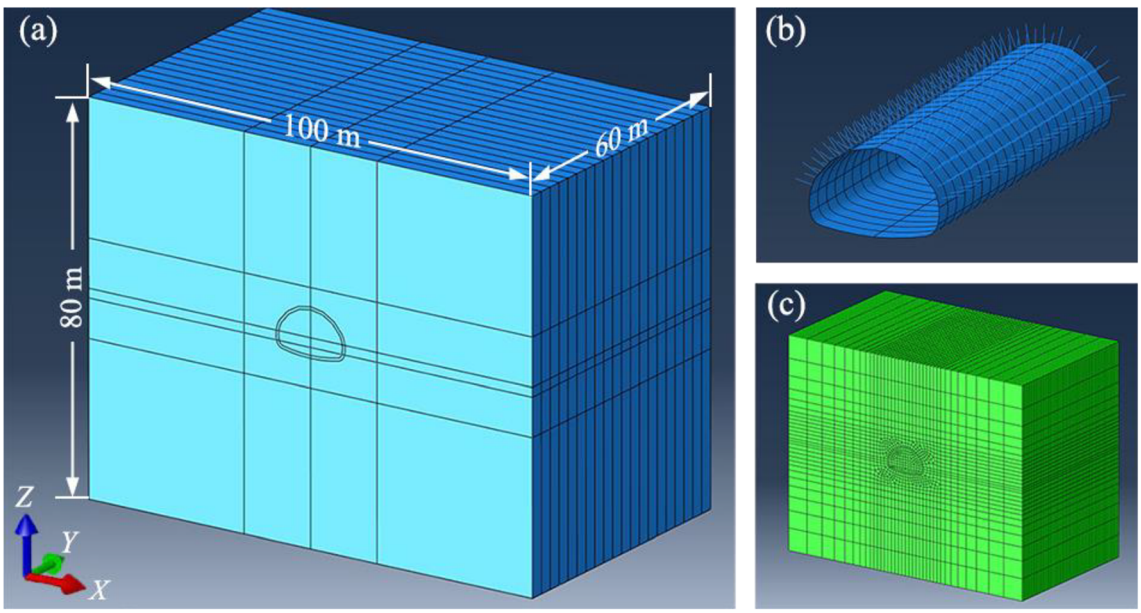

Fig. 10 **a** Numerical model of LK2+820 tunnel section. **b** Support system. **c** Mesh of model

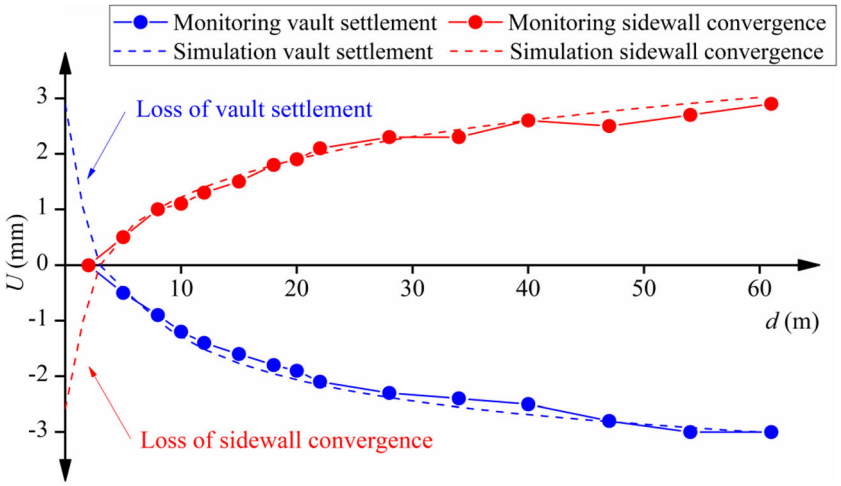

Fig. 11 Comparison of monitoring and simulation displacement curves for LK2+820 tunnel section

the quality of the training set, which is determined by the arrangement and number of samples, plays a vital role in the accuracy of the algorithm. In many studies, the high precision of the method is supported by a large number of training samples—up to hundreds or even thousands (Xue and Xiao 2017; Qi and Fourie 2018). One of the advantages of the proposed method is that although trained using relatively few samples (25 samples in this study), the error in prediction is still acceptable within the range of the parameters. However, the error can be large if some of the parameters required for the prediction lie outside the predefined range. Extending the parameter range may improve the compatibility. However, more samples have to be set to ensure precision, necessitating further simulation and prolonging the calculations. In addition, the stability of the proposed method must be improved because obtaining a stable average through multiple calculations is also time-consuming.

For predicting rock parameters using the intelligent algorithm for the excavation of tunnels, further studies will be required to focus on the following:

- Improving the prediction accuracy using few training samples—with the rapid development of the intelligent algorithm, new machine learning and optimization methods can be introduced in this field.
- Improving the stability of the algorithm—improved optimization algorithm could be employed to restrain the fluctuations in the results of the prediction.
- Verifying the applicability of the method in other cases of tunnel excavation—the excavation methods, the support system, and some other factors could also affect the

Table 9 Prediction results and relative errors obtained using PSO-ELM method for different testing samples

Testing sample		E (GPa)	μ	λ_x	H (10^2m)
Sample 1	Predefined value	2.60	0.32	1.24	1.05
	Back analysis value	2.668	0.332	1.251	1.073
	Relative error	2.62%	3.75%	0.89%	2.19%
	Average	2.36%			
Sample 2	Predefined value	3.40	0.33	1.32	0.95
	Back analysis value	4.323	0.333	1.329	1.124
	Relative error	27.15%	0.91%	0.68%	18.32%
	Average	11.76%			
Sample 3	Predefined value	4.50	0.34	1.46	1.08
	Back analysis value	4.389	0.325	1.426	1.111
	Relative error	2.47%	4.41%	2.33%	2.87%
	Average	3.02%			

E is the elastic modulus; μ is the Poisson's ratio; H is the burial depth; λ_x is the lateral pressure coefficient in x-direction, which is perpendicular to tunnel axis

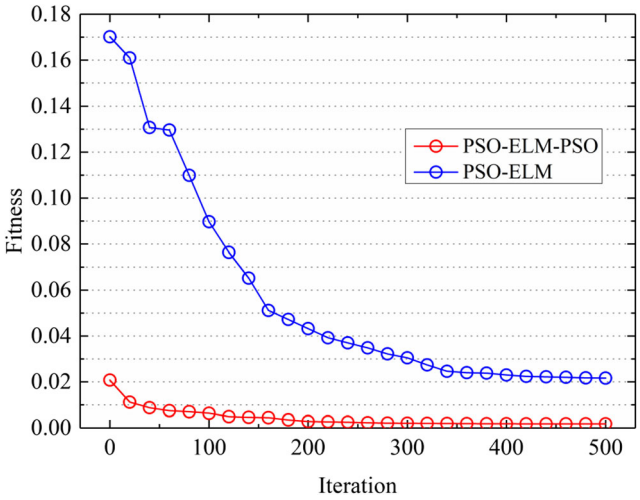

Fig. 12 Convergence of PSO-ELM-PSO and PSO-ELM algorithms in sample-learning procedure

displacement curve, leading to further discussions on parameter selection and data processing.

Conclusions

A displacement-based back analysis method characterized by the PSO-ELM-PSO algorithm is presented herein for estimating the rock parameters during tunneling. The considerations of displacement loss and space effect are reflected in the process of setting the input and output parameters. The case study and engineering application presented prove that this method can be well generalized, offer high precision, and be applied to other underground parameter estimations. The other primary conclusions drawn from this study are as follows:

(1) Owing to convenience in measurement, the monitoring distance is proven to be a suitable substitute for the monitoring time when recording the displacement data, both in simulation and practice. The loss in monitoring displacement is then correlated with the initial monitoring distance. Further, the space effect, which is usually reflected in the variations in displacement of the surrounding rock, is described by the key parameters of the curve-fitting function. Therefore, by selecting and processing the output parameters of the proposed algorithm, the displacement loss and space effect could be considered.

(2) The case study illustrates that the errors in the prediction of the rock parameters are all below 5% for the different testing samples, and that the simulation displacement curves match the real curves well. The displacement loss occurring before the construction of the lining accounts for 20–30% of the total displacement. The relative errors in the rock parameters with relatively larger sensitivities usually remain small and stable with the changes in the monitoring parameters. Further, to improve the prediction accuracy, it is suggested to select the rock parameters with large sensitivities as the inputs and typical monitoring values as the outputs when setting the training samples for displacement-based back analysis.

(3) The prediction results for the LK2+820 section in the Jigongshan Tunnel indicate that the proposed back analysis method, along with the PSO-ELM-PSO algorithm, could be suitably applied to engineering applications to predict the rock parameters and displacement loss. Moreover, as verified by the results of the field measurement, this method could offer an alternative approach for the estimation of ground stress.

(4) Comparisons between the PSO-ELM-PSO and PSO-ELM algorithms demonstrate that the quality of training samples is significant for the accuracy of the algorithm. Conducting orthogonal design when arranging the training set could help improve the quality of the learning samples and the precision of the algorithm. Further research is required to improve the stability and applicability of the method using few training samples.

Acknowledgements Much of the work described in this paper was supported by the National Natural Science Foundation of China under Grant Nos. 41725012 and 41931289, and the Shanghai Science and Technology Innovation Action Plan under Grant No. 18DZ1204402. The writers would like to greatly acknowledge all these financial supports and express their most sincere gratitude.

Code availability Not applicable.

Author contribution Conceptualization: Shi-jin Feng; methodology: Yong Zhao; writing—original draft: Yong Zhao; writing—review and editing: Shi-jin Feng; supervision: Shi-jin Feng.

Funding This work was supported by the National Natural Science Foundation of China under Grant Nos. 41725012 and 41931289, and the Shanghai Science and Technology Innovation Action Plan under Grant No. 18DZ1204402.

Data Availability The datasets used or analyzed during the current study are available from the corresponding author on reasonable request.

Declarations

Conflict of interest The authors declare no competing interests.

References

Bertuzzi R (2017) Back-analysing rock mass modulus from monitoring data of two tunnels in Sydney, Australia. J Rock Mech Geotech Eng 9:877–891. https://doi.org/10.1016/j.jrmge.2017.05.005

Cai M (2011) Rock mass characterization and rock property variability considerations for tunnel and cavern design. Rock Mech Rock Eng 44:379–399. https://doi.org/10.1007/s00603-011-0138-5

Cao J, Lin Z, Huang GB (2012) Self-adaptive evolutionary extreme learning machine. Neural Process Lett 36:285–305. https://doi.org/10.1007/s11063-012-9236-y

Eberhart RC, Kennedy J (1995) A new optimizer using particle swarm theory. Proceedings of the Sixth International Symposium on Micro Machine and Human Science. Nagoya, Japan, pp 39–43. https://doi.org/10.1109/MHS.1995.494215

Fakhimi A, Salehi D, Mojtabai N (2004) Numerical back analysis for estimation of soil parameters in the Resalat Tunnel project. Tunn Undergr Space Technol 19:57–67. https://doi.org/10.1016/S0886-7798(03)00087-7

Feng XT, Zhang Z, Qian S (2000) Estimating mechanical rock mass parameters relating to the Three Gorges Project permanent shiplock using an intelligent displacement back analysis method. Int J Rock Mech Min Sci 37:1039–1054. https://doi.org/10.1016/S1365-1609(00)00035-6

Feng X, Zhao H, Li S (2004) Modeling non-linear displacement time series of geo-materials using evolutionary support vector machines. Int J Rock Mech Min Sci 41:1087–1107. https://doi.org/10.1016/j.ijrmms.2004.04.003

Feng SJ, Zhao Y, Zhang XL, Bai ZB (2020) Leachate leakage investigation, assessment and engineering countermeasures for tunneling underneath a MSW landfill. Eng Geol 265:105447. https://doi.org/10.1016/j.enggeo.2019.105447

Gao W, Ge M (2016) Back analysis of rock mass parameters and initial stress for the Longtan tunnel in China. Eng Comput 32:497–515. https://doi.org/10.1007/s00366-015-0428-8

Gao X, Yan EC, Yeh TCJ, Yin XM, Cai JS, Hao YH (2020) Back analysis of displacements for estimating spatial distribution of viscoelastic properties around an unlined rock cavern. Comput Geotech 126:103724. https://doi.org/10.1016/j.compgeo.2020.103724

Hisatake M, Hieda Y (2008) Three-dimensional back-analysis method for the mechanical parameters of the new ground ahead of a tunnel face. Tunn Undergr Space Technol 23:373–380. https://doi.org/10.1016/j.tust.2007.06.006

Hoek E, Diederichs MS (2006) Empirical estimation of rock mass modulus. Int J Rock Mech Min Sci 43:203–215. https://doi.org/10.1016/j.ijrmms.2005.06.005

Huang GB, Zhu QY, Siew CK (2004) Extreme learning machine: a new learning scheme of feedforward neural networks. Neural Netw 2: 985–990. https://doi.org/10.1109/IJCNN.2004.1380068

Huang GB, Zhu QY, Siew CK (2006) Extreme learning machine: theory and applications. Neurocomputing 70:489–501. https://doi.org/10.1016/j.neucom.2005.12.126

Huang K, Liu B, Peng J, Peng D, Ding G, Wang Y (2011) Intelligent back-analysis of tunnel surrounding rock displacement based on genetic algorithm and neural network. J Cent South Univ (Sci Technol) 42:213–219 (in Chinese)

Jahed Armaghani D, Kumar D, Samui P, Hasanipanah M, Roy B (2020) A novel approach for forecasting of ground vibrations resulting from blasting: modified particle swarm optimization coupled extreme learning machine. Eng Comput. https://doi.org/10.1007/s00366-020-00997-x

Kaiser PK, Zou D, Lang PA (1990) Stress determination by back-analysis of excavation-induced stress changes—a case study. Rock Mech Rock Eng 23:185–200. https://doi.org/10.1007/BF01022953

Kang K, Hu N, Sin C, Rim S, Han E, Kim C (2017) Determination of the mechanical parameters of rock mass based on a GSI system and displacement back analysis. J Geophys Eng 14:939–948. https://doi.org/10.1088/1742-2140/aa6e78

Kavanagh KT, Clough RW (1971) Finite element applications in the characterization of elastic solids. Int J Solids Struct 7:11–23. https://doi.org/10.1016/0020-7683(71)90015-1

Liu K, Liu B (2019) Intelligent information-based construction in tunnel engineering based on the GA and CCGPR coupled algorithm. Tunn Undergr Space Technol 88:113–128. https://doi.org/10.1016/j.tust.2019.02.012

Lu AZ, Zhang N, Kuang L (2014) Analytic solutions of stress and displacement for a non-circular tunnel at great depth including support delay. Int J Rock Mech Min Sci 70:69–81. https://doi.org/10.1016/j.ijrmms.2014.04.008

Luo Y, Chen J, Chen Y, Diao P, Qiao X (2018) Longitudinal deformation profile of a tunnel in weak rock mass by using the back analysis method. Tunn Undergr Space Technol 71:478–493. https://doi.org/10.1016/j.tust.2017.10.003

Manzanal D, Drempetic V, Haddad B, Pastor M, Martin Stickle M, Mira P (2016) Application of a new rheological model to rock avalanches: an SPH approach. Rock Mech Rock Eng 49:2353–2372. https://doi.org/10.1007/s00603-015-0909-5

Mohapatra P, Chakravarty S, Dash PK (2015) An improved cuckoo search based extreme learning machine for medical data classification. Swarm Evol Comput 24:25–49. https://doi.org/10.1016/j.swevo.2015.05.003

Qi C, Fourie A (2018) A real-time back-analysis technique to infer rheological parameters from field monitoring. Rock Mech Rock Eng 51:3029–3043. https://doi.org/10.1007/s00603-018-1513-2

Rechea C, Levasseur S, Finno R (2008) Inverse analysis techniques for parameter identification in simulation of excavation support systems. Comput Geotech 35:331–345. https://doi.org/10.1016/j.compgeo.2007.08.008

Sakurai S, Takeuchi K (1983) Back analysis of measured displacements of tunnels. Rock Mech Rock Eng:173–180. https://doi.org/10.1007/BF01033278

Satapathy P, Dhar S, Dash PK (2017) An evolutionary online sequential extreme learning machine for maximum power point tracking and control in multi-photovoltaic microgrid system. Renew Energy Focus 21:33–53. https://doi.org/10.1016/j.ref.2017.08.001

Sharifzadeh M, Tarifard A, Moridi MA (2013) Time-dependent behavior of tunnel lining in weak rock mass based on displacement back analysis method. Tunn Undergr Space Technol 38:348–356. https://doi.org/10.1016/j.tust.2013.07.014

Shreedharan S, Kulatilake PHSW (2015) Discontinuum–equivalent continuum analysis of the stability of tunnels in a deep coal mine using the distinct element method. Rock Mech Rock Eng 49:1903–1922. https://doi.org/10.1007/s00603-015-0885-9

Song Z, Jiang A, Jiang Z (2015) Back analysis of geomechanical parameters using hybrid algorithm based on difference evolution and extreme learning machine. Math Probl Eng 2015:1–11. https://doi.org/10.1155/2015/821534

Wu C, Hong Y, Chen Q, Karekal S (2019) A modified optimization algorithm for back analysis of properties for coupled stress-seepage field problems. Tunn Undergr Space Technol 94:103040. https://doi.org/10.1016/j.tust.2019.103040

Xu J, Ni Y (2019) Displacement ratio dichotomy back analysis of surrounding rock-initial support system of weathered rock tunnel. Arab J Geosci 12:181. https://doi.org/10.1007/s12517-019-4334-z

Xue X, Xiao M (2017) Deformation evaluation on surrounding rocks of underground caverns based on PSO-LSSVM. Tunn Undergr Space Technol 69:171–181. https://doi.org/10.1016/j.tust.2017.06.019

Xue Y, Bai C, Qiu D, Kong F, Li Z (2020) Predicting rockburst with database using particle swarm optimization and extreme learning machine. Tunn Undergr Space Technol 98:103287. https://doi.org/10.1016/j.tust.2020.103287

Yang Z, Liu Z, Wang S (1983) A practical back-analysis method from displacements to estimate some parameters of rock mass for design of an underground opening. Proceeding of International Symposium on Field Measurements in Geomechanics. Zurich, Switzerland, pp 1267–1276

Yazdani M, Sharifzadeh M, Kamrani K, Ghorbani M (2012) Displacement-based numerical back analysis for estimation of rock mass parameters in Siah Bisheh powerhouse cavern using continuum and discontinuum approach. Tunn Undergr Space Technol 28: 41–48. https://doi.org/10.1016/j.tust.2011.09.002

Zhang LQ, Yue ZQ, Yang ZF, Qi JX, Liu FC (2006) A displacement-based back-analysis method for rock mass modulus and horizontal in situ stress in tunneling – illustrated with a case study. Tunn Undergr Space Technol 21:636–649. https://doi.org/10.1016/j.tust.2005.12.001

Zhang C, Feng X, Zhou H, Hou J, Su G (2009) Method of obtaining loss convergence displacement and its application to tunnel engineering. Rock Soil Mech 30:997–1003+1012 (in Chinese)

Zhang Z, Li X, Li Y (2017) Uniqueness of displacement back analysis of a deep tunnel with arbitrary cross section in transversely isotropic rock. Int J Rock Mech Min Sci 97:110–121. https://doi.org/10.1016/j.ijrmms.2017.04.008

Zhang Y, Su G, Liu B, Li T (2020a) A novel displacement back analysis method considering the displacement loss for underground rock mass engineering. Tunn Undergr Space Technol 95:103141. https://doi.org/10.1016/j.tust.2019.103141

Zhang P, Wu H, Chen R, Chan THT (2020b) Hybrid meta-heuristic and machine learning algorithms for tunneling-induced settlement prediction: a comparative study. Tunn Undergr Space Technol 99: 103383. https://doi.org/10.1016/j.tust.2020.103383

Zhou C, Yin K, Cao Y, Ahmed B (2016) Application of time series analysis and PSO–SVM model in predicting the Bazimen landslide in the Three Gorges Reservoir, China. Eng Geol 204:108–120. https://doi.org/10.1016/j.enggeo.2016.02.009